LASER PHYSICS LETTERS

www.lphys.org

WILEY-VCH

Abstract: We report the use of optical coherence tomography (OCT) to detect and quantify demineralization process induced by S. *mutans* biofilm in third molars human teeth. Artificial lesions were induced by a S. *mutans* microbiological culture and the samples (N = 50) were divided into groups according to the demineralization time: 3, 5, 7, 9, and 11 days. The OCT system was implemented using a light source delivering an average power of 96 μW in the sample arm, and spectral characteristics allowing 23 μm of axial resolution. The images were produced with lateral scans step of 10 μm and analyzed individually. As a result of the evaluation of theses images, lesion depth was calculated as function of demineralization time. The depth of the lesion in the root dentine increased from 70 μm to 230 μm (corrected by the enamel refraction index, 1.62 @ 856 nm), depending of exposure time. The lesion depth in root dentine was correlated to demineralization time, showing that it follows a geometrical progression like a bacteria growth law.

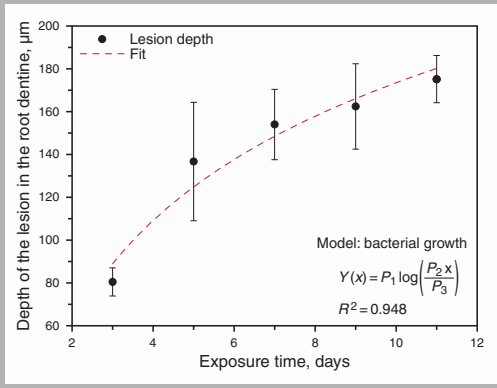

Progression of lesion depth in root dentine as function of exposure time, showing that it follows a geometrical progression like a bacteria growth law

Determination of dental decay rates with optical coherence tomography

A.Z. Freitas, [1,*] *D.M. Zezell,* [1] *M.P.A. Mayer,* [2] *A.C. Ribeiro,* [2] *A.S.L. Gomes,* [3] *and N.D. Vieira, Jr.* [1]

[1] Nuclear and Energy Research Institute, IPEN-CNEN/SP, Av. Lineu Prestes, 2242, - CEP: 05508-900, São Paulo/SP, Brazil
[2] University of São Paulo, Institute of Biomedical Sciences: Av. Prof. Lineu Prestes, 2415 CEP: 05508-900, São Paulo/SP, Brazil
[3] Graduate Program in Odontology and Physics Department, Universidade Federal of Pernambuco, Cidade Universitria, 50670-901, Recife/PE, Brazil

Received: 26 July 2009, Revised: 8 August 2009, Accepted: 11 August 2009
Published online: 26 August 2009

Key words: optical coherence tomography; caries lesion; diagnostic imaging; backscattering

PACS: 42.30.Wb, 42.62.Be, 87.57.C-, 87.63.lt, 87.85.Pq, 87.85.Ng

1. Introduction

Optical coherence tomography (OCT) is a diagnostic imaging technology, in which the coherence features of light are exploited, leading to an imaging technology that is capable to produce high resolution cross-sectional images of the internal microstructure of living tissue. Its applications in medicine were reported less than a decade ago [1–3], but its root lie in early works on white-light interferometry, that led to the development of optical coherence-domain reflectometry (OCDR), an one dimensional (1-D) optical ranging technique [4].

Although OCDR was originally developed to identify faults in optic fiber cables and network components, its capability to probe the human eye structure [5,6] and other biological tissues [7,8] was readily recognized. Some optical methods can evaluate skin physiology [9] and functionality, in particular is possible to associate a Doppler OCT to monitor flow velocity distribution [10], and permeability of arterial tissue to glucose [11].

The optical sectioning ability of OCT, due to the short temporal coherence of a broadband light source, enables OCT scanners to image microscopic tissue structures at depths beyond the conventional bright-field and confocal

* Corresponding author: e-mail: freitas.az@ipen.br

microscopes. The absorption and scattering properties of biological tissues are the main limiting factor for depth penetration of OCT, but it can be improved applying an optical clearing [12, 13].

Commonly, dentists evaluate the oral health of a patient through three main methods: visual, tactil examination and radiographic imaging [14]. The visual method can not detect early caries lesion and depends of the dentist ability to identify these lesions. There are many caries detector dyes commercially available purported to aid the dentist in differentiation of infected tissue, but they are not specific and would result in unnecessary removal of sound tooth structure [15]. Optical methods like transillumination, both in the visible [16] and near infrared [17], as well as laser fluorescence [18, 19] have also been proposed, a recent work shows that is possible to detect early caries using LEDs in ultraviolet spectral range [20], however none of them can precisely detect the caries lesion position. Radiographies may reveal structural characteristics of teeth and bone that can not be identified by direct visual examination, and are sensitive to detecting regions of significant carious demineralization. In addition, radiography uses potentially harmful ionizing radiation. Furthermore, the methods for dental caries detection currently available are mostly qualitative, and there is a need of a quantitative, non-destructive method to measure mineral loss. OCT in dentistry has been recently used to *in vitro* studies evaluating enamel interface restoration [21], early caries diagnostics [22], and analysis of the performance of dental materials [23]. In 2006, the first OCT image of dental pulp was performed using rat's teeth [24], and more recently, remaining dentin and pulp chamber from human's teeth were also imaged by OCT *in vitro* [25].

The goal of this work was to use the OCT technique ability to produce *in vitro* tomographic images of dental microstructure, measure caries lesion depth after *in vitro* demineralization induced by S. *mutans* biofilm and determine mathematical progression law.

2. Methodology

2.1. System configuration

The configuration employed in the OCT system was the "open air" Michelson interferometer illustrated in Fig. 1. In this type of interferometer, light from the source is divided by a 50:50 beam-splitter, where half of the optical intensity is transmitted by a delay line. The remaining half of the light is directed to the sample. A Ti:Sapphire laser (Mira – Coherent) was used in mode-locked regime running at 830 nm with 20 nm FWHM of spectral width (measured by a OSM2-400VS/NRU spectrometer, Newport) providing 23 μm of axial resolution.

The laser system provided an output average power of 100 mW (Ophir PowerMeter) at a repetition rate of 76 MHz, but only 96 μW was used in the sample arm.

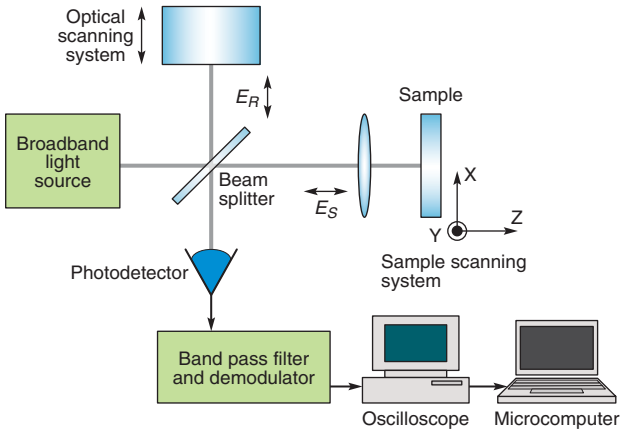

Figure 1 (online color at www.lphys.org) Main components of the OCT setup employed

The delay line was made by a fast Fourier scanning, consisting of a scanner (General Scanning 6120D) operating at 200 Hz, a grating with 590 lines/mm (p = 1.69 μm), 25×25 mm lateral dimensions, and a lens with 50 mm of focal length. The maximum angular excursion of the scanning mirror was set to produce an usable group delay scan of approximately lg = 1.5 mm. A low noise amplified detector (SR-194) adapted to a home made electronic circuit was used to detect only the positive part of signal. A digital oscilloscope (Tektronix 3000B) was employed to display data, which were stored into a personal computer. The precise displacement of the sample in the X-axis during the image acquisition was controlled by a computer controlled translation stage (Thorlabs, T25-XYZ) with minimum step of 0.05 μm.

2.2. Sample preparation

Twenty five human third molars were used in this study. After the surgical procedure, teeth were cleaned under tap water to remove the organic debris. Then, they were immersed in deionized water and kept under refrigeration until use.

The teeth were longitudinally cut through the mesiodistal direction, resulting in 50 samples. The surfaces were cleaned up, dried and covered with acid resistant varnish except at the rectangular windows (2×4 mm), as shown in Fig. 2.

A total of 111 windows were submitted to the demineralization process for different experimental times, distributed at different sites along buccal and lingual surfaces: enamel (n = 36), enamel-cementum junction (n = 58) and dentine root surface (n = 17). Each sample was individually fixed at the bottom of the wells of a 24 acrylic culture plate and sterilized by gamma rays (25 KGy, Gammacell/Ipen).

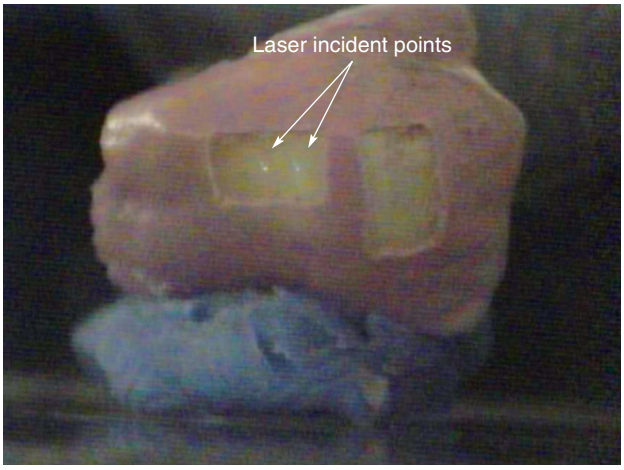

Figure 2 (online color at www.lphys.org) Frame of video image captured showing demineralization window. The laser incidence points were used to define the position of OCT scan region, for optical microscopy analysis

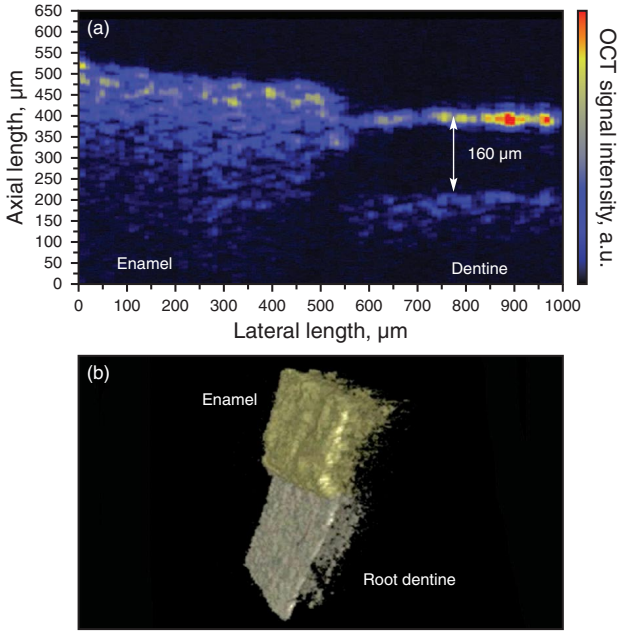

Figure 3 (online color at www.lphys.org) (a) – transversal OCT image after the sample was submitted to the demineralization process for 11 days and (b) – its image reconstruction in 3D, that allows another image sections analysis different from those obtained directly from the OCT system

2.3. Microbiological procedure

Samples were submitted to demineralization induced by *Streptococcus mutans* (GS5) biofilm. Bacteria were previous cultured in Brain Heart Infusion Agar during 48 h at 37°C with 5% CO_2. One single colony was transferred to trytic soy broth, supplemented with 5% sucrose with 0.01% of potassium tellurite, and submitted to the same culture conditions mentioned above for 16 h. The concentration of the bacterial suspension was adjusted to 0.5 at 660 nm. Inoculation occurred at the first day with 3 mL of the adjusted bacterial suspension. Samples were incubated at 37°C with 5% CO_2 during all the experimental time. Broth was renewed every 48h carefully to not disturb the biofilm structure at the top surface of the samples. At the end of each demineralization time, samples were removed from the wells and analyzed by OCT before be prepared to microscopy analysis.

2.4. Microscopic analysis

After OCT analysis, the formation of caries-like lesions was evaluated by polarized light microscopy. The operator used snapshot video image showing the laser incident points (Fig. 2) as reference to place the diamond disk approximately at the same point analyzed by OCT. Sections were performed perpendicularly to sample surface and resulted slices (400 μm of thickness) were washed with distilled water. Afterwards, they were immersed in quinoline (SIGMA) for at least 2 hours before being analyzed under the microscope by polarization light at 50× (Leika DMLP). The microscope images were captured by a digital camera and the lesion depth measured with a software program (Image J v1.3).

2.5. Image formation

The OCT cross section images, e.g. Fig. 3a, were constructed using the depth-priority scanning protocol (A-scan), where axial scans were acquired at successive transverse positions. The tooth was moved laterally, perpendicular to the laser axis, in 10 μm increments. All scans were normalized to the maximum OCT signal (front surface) and a false-color gray scale was used [22]. To obtain the results showed in Fig. 3b, transverse images sections from different positions of the sample in the Y-axis (see Fig. 1) were stacked together. The construction was accomplished with the aid of analysis software and voxel visualization (VGStudio Max 1.2). This three-dimensional reconstruction allows transversal sections analysis different from those directly obtained from the OCT system.

3. Results and discussion

The OCT images produced confirmed that it is possible to clearly depict internal structure of dental tissue and detect early artificial caries. Fig. 3a exhibits the structure of a representative caries lesion after 11 days of demineralization. It is possible to visualize subsurface lesion in enamel

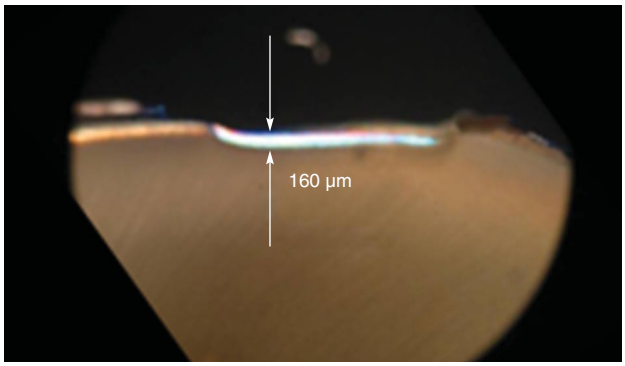

Figure 4 (online color at www.lphys.org) Visible polarized micrograph of sample after 11 days of demineralization, showing caries region

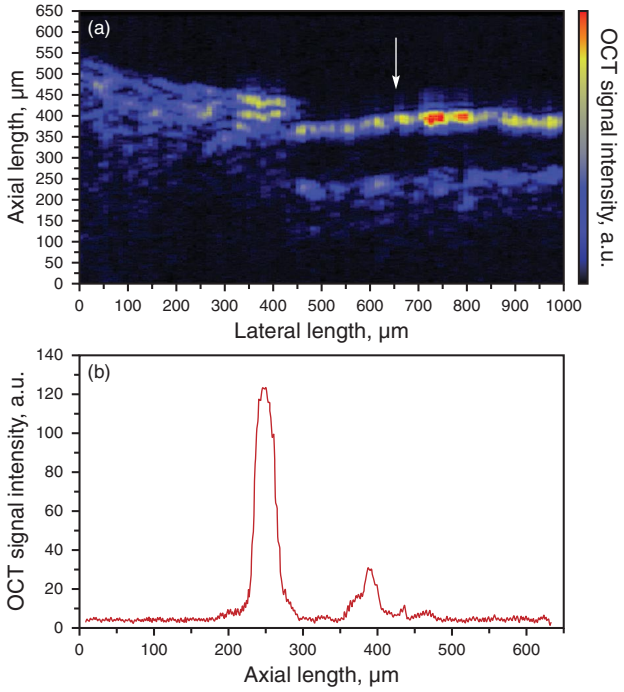

Figure 5 (online color at www.lphys.org) OCT image at enamel-cementum junction for teeth after 7 days of demineralization. Notice lesion depth, and the OCT signal for cementum region indicated by an arrow

surface, on the left side of the figure, while cementum surface reveals small backscattering signal between the tooth surface and the body of lesion, which is visualized on the right side of figure.

Lesion depth was measured in the images between the tooth surface and the back of body lesion and corrected by tooth refraction index (1.62 @ 856nm) [16]. The results obtained by OCT were in agreement with the optical microscope image shown in Fig. 4.

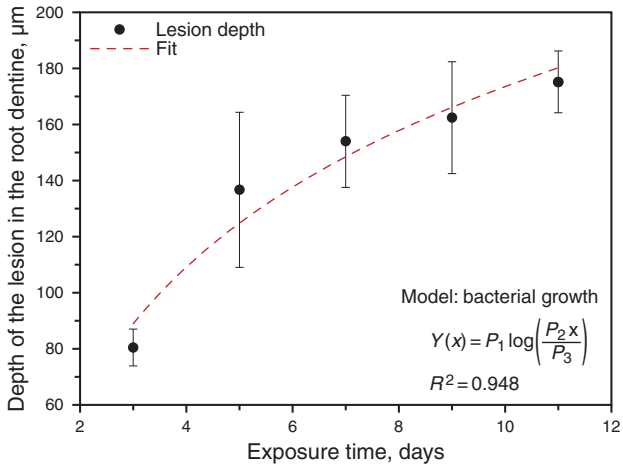

Figure 6 (online color at www.lphys.org) Progression of lesion depth in root dentine as function of exposure time, showing that it fits a geometrical progression like a bacteria growth law

The cross section optical coherence tomographic images clearly show demineralization process taking place in the sample as function of exposure time to bacteria culture. Caries region have deeper signal than sound region and its intensity is directly related with demineralization time. The mineral loss reduces the backscattering coefficient, allowing a larger penetration of the laser beam in to the sample. The OCT images for all the samples were generated, showing the progression of the caries lesion process by the time. Fig. 5 shows the cross section image of a sample after 7 days of demineralization and a single axial scan line. The distances measured in the OCT images from tooth surface to the back limit of body lesion, for different time of demineralization are shown in Fig. 6. The data fits very well in a logarithm function $Y(x) = P_1 \log(P_2 x / P_3)$ following a typical bacteria growth law, where P_1, P_2, and P_3 are adjustable parameters.

Bacterial population growing exponentially by binary fission follows a geometric progression, and can be represented by: $b = B \cdot 2^n$, where b is the number of bacteria at the end of time interval, B is the number of bacteria at the beginning of time interval, and n is the number of generations (number of times that cell population doubles during the time interval). Solving for n, the equation becomes:

$$n = \frac{\log b - \log B}{\log 2} \approx 3.3 \log \frac{b}{B} . \qquad (1)$$

This exponential growth cannot be continued for long period in a batch culture [26] (e.g. a closed system such as a test tube or flask). Population growth is limited by one of three factors:

1. exhaustion of available nutrients;
2. accumulation of inhibitory metabolites or end products;
3. exhaustion of space, in this case called a lack of "biological space".

During the stationary phase, if viable cells are being counted, it cannot be determined whether some cells are dying and an equal number of cells are dividing, or if the population of cells just stopped growing and dividing.

In this work the experimental model is based in a progression of lesion depth following a geometrical progression like a bacteria growth law. To the best of our knowledge this is the first time that this relation is presented. In the literature one can find a relation between the number of cycle of demineralization/remineralization and the integrated reflectivity of surface, that demonstrate the linear relation when the root square of time is considered [27–29]. Of course, caries progression and severity may not fit exactly this law because the process *in vivo* is much more complex, involving dynamic of ions, as calcium and phosphorus, which are uptake and release from solution. However, it can seen that the data follows the same theoretical behavior. Another possibility for this behavior is a crystal growth in solution, and this hypothesis is now under study.

4. Conclusions

The OCT system provides a powerful contact less and non-invasive diagnostic method, that could be used to complement, the traditional diagnostic methods such as X-ray radiography, avoiding potentially hazardous ionization radiation.

In this work an OCT system with a fast-Fourier scan delay line was implemented with average power of 96 μW in the sample arm, and a 23 μm of axial resolution. In particular it was shown due to its spatial resolution and contrast that it is possible to detect early artificial caries induced by S. *mutans* culture. The images generated by OCT made possible to determine the lesion depth as function of sample exposure time to microbiological culture (demineralization). We observed that the depth of the lesion in the root dentine increased from 70 μm to 230 μm, for 3 days to 11 days of demineralization time, and follows the bacterial population growth law. Further experiments are under way, taking into account other variables during the demineralization process like pH, population counting and crystal growth in solution, in order to explain the processes more precisely.

Acknowledgements The authors would like to acknowledge support from FAPESP (grant No. 00/15135-9), PROCAD (grant No. 0/15135-9), and partial support from Institute of Millenium in Nonlinear Optics, Photonics, and Biophotonics a CNPq/MCT program.

References

[1] J.G. Fujimoto, M.E. Brezinski, G.J. Tearney, S.A. Boppart, B. Bouma, M.R. Hee, J.F. Southern, and E.A. Swanson, Nature Med. **1**, 970–972 (1995).
[2] A.F. Fercher, C.K. Hitzenberger, W. Drexler, G. Kamp, and H. Sattmann, Am. J. Ophthalmol. **116**, 113–114 (1993).
[3] R.C. Youngquist, S. Carr, and D.E.N. Davies, Opt. Lett. **12**, 158–160 (1987).
[4] K. Takada, I. Yokohama, K. Chida, and J. Noda, Appl. Opt. **26**, 1603–1606 (1987).
[5] A.F. Fercher, K. Mengedoht, and W. Werner, Opt. Lett. **13**, 186–188 (1988).
[6] J.A. Izatt, M.R. Hee, E.A. Swanson, C.P. Lin, D. Huang, J.S. Schuman, C.A. Puliafito, and J.G. Fujimoto, Arch. Ophthalmol. **112**, 1584–1589 (1994).
[7] X. Clivaz, F. Marquis-Weible, R.P. Salathé, R.P. Novàk, and H.H. Gilgen, Opt. Lett. **17**, 4–6 (1992).
[8] J.M. Schmitt, A. Knüttel, and R.F. Bonner, Appl. Opt. **32**, 6032–6042 (1993).
[9] J. Lademann, A. Patzelt, M. Darvin, H. Richter, C. Antoniou, W. Sterry, and S. Koch, Laser Phys. Lett. **5**, 335–346 (2008).
[10] B. Veksler, E. Kobzev, M. Bonesi, and I. Meglinski, Laser Phys. Lett. **5**, 236–239 (2008).
[11] K.V. Larin, M.G. Ghosn, S.N. Ivers, A. Tellez, and J.F. Granada, Laser Phys. Lett. **4**, 312–317 (2007).
[12] I.V. Larina, E.F. Carbajal, V.V. Tuchin, M.E. Dickinson, and K.V. Larin, Laser Phys. Lett. **5**, 476–479 (2008).
[13] S.G. Proskurin and I.V. Meglinski, Laser Phys. Lett. **4**, 824–826 (2007).
[14] B. Angmar-Mansson and J.J. Ten Bosh, Adv. Dent. Res. **7**, 70–79 (1993).
[15] D. McComb, J. Can. Dent. Assoc. **66**, 195–198 (2000).
[16] A. Wenzel, E.H. Verdonschot, G.J. Truin, and K.G. Konig, J. Dent. Res. **71**, 1934–1937 (1992).
[17] R. Jones, G. Huynh, G. Jones, and D. Fried, Opt. Express **11**, 2259–2265 (2003).
[18] D. McComb and L.E. Tam, J. Can. Dent. Assoc. **67**, 454–457 (2001).
[19] J. Kühnisch, K. Bücher, and R. Hickel, J. Dent. **35**, 509–512 (2007).
[20] D. Bakhmutov, S. Gonchukov, O. Kharchenko, O. Voytenok, and B. Zubov, Laser Phys. Lett. **5**, 375–378 (2008).
[21] L.S.A. de Melo, R.E. de Araujo, A.Z. Freitas, D. Zezell, N.D. Vieira, Jr., J. Girkin, A. Hall, M.T. Carvalho, and A.S.L. Gomes, J. Biomed. Opt. **10**, 064027 (2005).
[22] A.Z. Freitas, D.M. Zezell, N.D. Vieira, Jr., A.C. Ribeiro, and A.S.L. Gomes, J. Appl. Phys. **99**, 024906 (2006).
[23] A.K.S. Braz, B.B.C. Kyotoku, R. Braz, and A.S.L. Gomes, Dent. Mater. **25**, 74–79 (2009).
[24] C.M.F. Kauffman, M.T. Carvalho, R.E. Araujo, A.Z. Freitas, D.M. Zezell, and A.S.L. Gomes, Proc. SPIE **6137**, 613707 (2006).
[25] D.D.D. Fonsêca, B.B.C. Kyotoku, A.M.A. Maia, and A.S.L. Gomes, J. Biomed. Opt. **14**, 024009 (2009).
[26] D.K. Button, Microbiol. Rev. **49**, 270–297 (1985).
[27] D. Fried, J. Xie, S. Shafi, J.D.B. Featherstone, T.M. Breunig, and C. Le, J. Biomed. Opt. **7**, 618–627 (2002).
[28] R.S. Jones, M. Staninec, and D. Fried, J. Biomed. Opt. **9**, 1297–1304 (2004).
[29] J.D.B. Featherstone, J.M. ten Cate, M. Shariati, and J. Arends, Caries Res. **17**, 385–391 (1983).